Diyala Journal of Engineering Sciences

Journal homepage: https://djes.info/index.php/djes

ISSN: 1999-8716 (Print); 2616-6909 (Online)

Structural Behavior of Reinforced Concrete Columns Fully and Partially Reinforced with GFRP Bars Tested under Concentric or Eccentric Compressive Loads

Mohammed S. Irhayyim*, Wisam A. Aules and Muyasser M. Jomaa'h

Department of Civil Engineering, Tikrit University, P. O. Box 42, Tikrit, Salah Al-Din, 34001, Iraq

ARTICLE INFO

Article history:
Received May 11, 2024
Revised August 12, 2024
Accepted August 15, 2024
Available online September 1, 2024

Keywords:
Concrete Columns
GFRP bars
Partially Reinforcement
Concentric Load
Eccentric Load

ABSTRACT

Concrete columns reinforced with glass fiber-reinforced polymer (GFRP) bars have been greatly interesting recently. The distinct properties of GFRP bars, such as high tensile strength and low modulus of elasticity compared to steel bars, as well as the linear stress-strain behavior, make the study of GFRP-reinforced concrete (FRP-RC) columns important. This paper investigates the structural behavior of column specimens reinforced by fully and partially GFRP bars subjected to concentric and eccentrically applied Compressive loads. 12 columns were reinforced by (36%, 64%, and 100%) of the GFRP bars ratio, and the control specimen was reinforced by conventional steel rebars; all specimens were tested under different eccentric ratios (e/h) 0, 0.66, and 1. The failure mode, the relation between the axial load and the average axial displacement, and a comparison between the experimental results and the theoretical interaction diagram for columns were presented and discussed. The results show that most of the failure in specimens occurs as a compressive failure, and it fails in the weakest region by crushing concrete, as well as kinking in GFRP bars. Using GFRP bars significantly increases the axial displacement values compared to the steel rebars in longitudinal reinforcement and decreases the failure load for specimens with an increase in the ratio of GFRP bars. The average axial displacement value for columns specimens tested under eccentric load at e/h equal to 0.66 and 1 decreases by 75% and 94.4% compared with the control specimen. Moreover, the theoretical and experimental results for the pure axial load capacity were in good agreement. The failure loads for columns with partial reinforcement are higher than fully replacement with GFRP bar.

1. Introduction

Reinforced Concrete (R.C.) columns are structural members used mainly to carry compression loads. They are conventionally composed of steel reinforcing cages embedded in concrete [1,2].

Fiber-reinforced polymer (FRP) bars have been used in the construction industry as an alternative to traditional steel reinforcing bars in concrete structures where high corrosion resistance, high tensile strength, and low weight are demanded [3]. FRP composites have been used in various structural members such as beams, deep beams, corbels, dapped ends, slabs, walls, etc. [4–14]. As a result, GFRP bars have become widespread in structural applications where bending capacity and high tensile strength are needed. However, applying GFRP bars in concrete columns has been limited and less than in other concrete applications [15]. However, different studies have been conducted

* Corresponding author.
E-mail address: mohmmed_sabah91@yahoo.com
DOI: 10.24237/djes.2024.17305

on GFRP bars in columns [16–21]. It is commonly believed that GFRP bars are not as effective as steel bars in the load-bearing capacity of concrete columns. Because GFRP bars have low strength to compressive stresses. In addition, these bars have high tensile strength to compressive strength, unlike traditional steel rebars, whose compressive and tensile strength are close. Therefore, in design, ACI 440.1R [22] neglects the rebar's contribution in compression and allows its replacement with concrete.

Canadian standard for the design and construction of building structures with GFRP CAN/CSA S806 code [22] allows the use of GFRP rebars in concentrically loaded columns only if the designer neglects their contribution to strength. That means GFRP reinforcement shall not be used as longitudinal reinforcement in structural members subjected to combined loaded flexure and compressive axial load. In cases where these structural members are reinforced longitudinally with steel bars, the requirements of CSA Standard A23.3 shall apply to the steel reinforcement, and Clauses CSA Standard 8.4.3.2 and CSA Standard 8.4.3.3 shall apply if it uses the GFRP as transverse reinforcement. based on this statement, the existing GFRP bars in the column under concentric load do not add any extra compressive strength to the column, Motavalli. et al. [23] mentioned that since the contribution of the compressive GFRP rebars to the load-carrying capacity of concrete columns is less than the steel rebars, their contribution is ignored.

Previous studies have been conducted on column reinforcement by GFRP bars [18,24–28] and the strength of these bars to corrosion compared to steel rebars [29–32], It has been shown through studies that GFRP bars have shown excellent corrosion resistance. Consequently, the stress-strain relationship of GFRP bars is nearly linear, lacking a yield point. It is advisable to reduce the ultimate tensile strength as the design criterion in comparison to normal steel. Columns reinforced with fully GFRP bars or reinforced partially were also studied under different loads (concentric or eccentric) to know the effect of the eccentricity ratio on load capacity [33–36], the failure mode of the eccentric column showed more ductile failure characteristics than the concentric column with the increase in eccentricity. Elchalakani and Guowei Ma [37], It was found that the average axial load-carrying capacity of GFRP RC columns was 93.5% of their steel RC column counterparts. It was also found that the GFRP RC columns under concentric load exhibited a 3.2% average increase in the load-carrying capacity concerning the plain concrete section capacity, Rusul Z. and Hassan F.[33] finding that Increasing the longitudinal reinforcement ratio from 1.6 % to 4.1 % marginalizes the load-carrying capacity of GFRP-RC columns subjected to concentric loading. In comparison, it significantly affects columns exposed to eccentric loading by increasing the ultimate capacity by 83.5 and 177.4 % for columns with tie spacing of 60 mm and (e/h = 0.21, 0.42), respectively. Also, 48.7 and 62.7 % for columns with 120 mm tie spacing. and It found that columns reinforcing with fully GFRP have the highest vertical displacement because of their lowest bearing capacity. The eccentric load of GFRP R.C. columns differ from that of steel-R.C. columns under a high eccentricity ratio (eccentricity-to-width ratio) [38–42]. The failure of column reinforcement with GFRP bars tested under high eccentric loading e/D was not high because of the rupture of the GFRP bars compared with column reinforcement by steel especially under a high eccentricity ratio. Benmokrane and hadhood [40] found an average loss in the ultimate load of 30, 50, 75, and 90% (compared with the concentric columns with steel rebars) were reported for columns tested under eccentricity-to-diameter ratios of 8.2, 16.4, 32.8, and 65.6%, respectively. The high eccentricity (e/h) ratio reduced the load capacity of specimens containing GFRP bars to a lesser extent than specimens containing conventional steel reinforcement [34,43–47].

Previous research has studied the effect of using GFRP bars as a full reinforcement in columns. Moreover, based on the author's knowledge, few studies were conducted on concrete columns partially reinforced with GFRP bars and subjected to two types of loads (concentric or eccentric). Therefore, this field in

need to provide more experimental studies to cover the uncertainty in design or analysis. In the present study, twelve reinforced concrete columns were tested. These specimens were reinforced with different ratios of reinforcement of GFRP bars (partially and fully reinforced) in ratios (36%, 64%, and 100%), as well as the control specimen for comparison was reinforced with conventional steel rebars. All specimens were tested under different eccentric ratios (e/h) 0, 0.66, and 1. The objective of this study is to evaluate the performance of these columns in terms of mode of failure, deformability, and a compression between the theoretical and experimental of the interaction diagram.

2. Experimental program

Twelve half-scale reinforced concrete column specimens were prepared for this investigation. The dimensions were 150 mm * 150 mm in cross-section and 1700 mm in height. These specimens were tested under concentric and eccentric loads. Table 4 shows the R.C. column specimens' groups, column coding, reinforcement ratios, eccentricity, and reinforcement details. The material properties, specimen details, and test setup will be illustrated in detail in the following sections.

2.1 Concrete

The concrete mix used in this study was the same for all specimens. The materials used in this concrete were river sand with fineness modulus (2.43), crushed stone with a maximum size of 19mm, ordinary Portland cement, and water. A concrete mix has been designed, and the suitable proportions of the mix ingredients satisfy the required compressive strength of 25 MPa in 28 days according to ACI code [48]. In Table 1 the average concrete compressive strength was determined at 7 days (19.86 MPa) and 28 days (29.72 MPa) based on testing three concrete cubes (150 mm * 150 mm * 150mm) according to BS EN 12390-1:2000. [49].

2.2. Reinforcements

2.2.1 Steel reinforcement rebars

Three types of deformed reinforcing steel bars were used in the present study. Steel rebars with Ø10, Ø8, and Ø6mm diameters were used for longitudinal reinforcement and corbel columns. Steel bars with diameters of Ø 8 mm were used as transverse ties for all columns. The mechanical properties of the steel rebars illustrated in Table 2 were obtained from the manufacturer.

2.2.2 Glass fiber reinforcement polymer bars (GFRP bars)

Fibers commonly used in FRP bars are glass, carbon, aramid, and basalt. Glass fiber reinforcement polymer (GFRP) offers an economical balance between specific strength properties and cost, which makes them the favorite in most RC applications [50–52]. The GFRP bars with diameters of 10, 8, and 6mm, as shown in Figure 1, were used for longitudinal reinforcement in columns; the properties of GFRP bars, according to the manufacturer datasheet, are summarized in Table 3.

Table 1: Results of compressive strength tests of the concrete mixtures design

NO. of mix	Age (days)	Proportions ACI-Code design	Compressive strength f_{cu} (MPa)	Average compressive strength f_{cu} (MPa)
1	7	1: 1.88: 2.76	20.41 19.91 20.36	19.86
2	28	1: 1.88: 2.76	28.67 28.34 29.39	29.72

Table 2: The tensile test results of the reinforcement steel bar

Diameter of steel bars (mm)	Elongation (%)	Yield stress (*Fy*) (MPa)	Ultimate strength (*Fu*) (MPa)
6	9.0	524	602
8	9.0	541	631
10	9.2	584	655

Table 3: Properties of glass fiber reinforcement polymer (GFRP) bars used according to manufactured data

Diameter of GFRP bars) mm)	Initial Area (mm^2) Initial Area (mm^2)	Density (G/gm^3)	Specific Gravity (gr/23° C)	Tensile Strength @ Break (MPa)	Elongation (%)
6	28.26	2085	2.094	1209	2.1
8	50.27	2086	2.094	1215	2.0
10	78.53	2085	2.093	1207	2.4

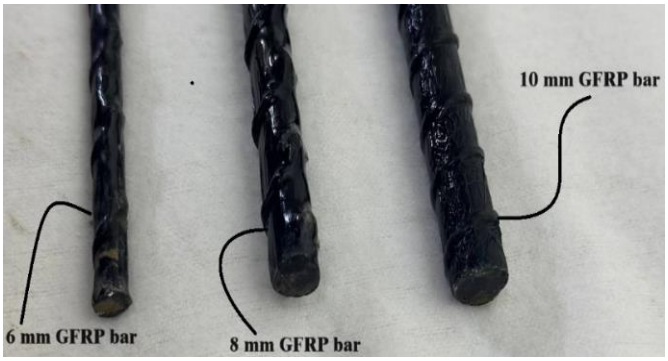

Figure 1. GFRP bars used

2.3 Preparing the specimens

According to the section on specimens, two types of wooden forms were used to prepare the columns. The first type had 4 forms for normal columns without corbel (N), and the second type had 8 forms for columns with corbel (C), as shown in Figure 2 .The length of the forms used in the study was (1700) mm, and the cross-section dimensions of the form at the supports (top and bottom) are (150×150) mm for normal concrete columns without corbel and 300 mm × 150 mm for columns with corbel. Figure 3 shows the reinforcement details and dimensions of the column without and with the corbel. Moreover, Table 4 illustrates the identification of each specimen. For example, samples N and C represent the column without and with corbel, respectively, and S and G represent the column reinforced with steel or GFRP bars. In addition, the replacement percentage of GFRP bars was indicated by the numbers 36 and 64. As well as the numbers 1 and 2 come after the letter C, representing the value of eccentricity 100 mm and 150 mm, respectively. Code details of the column specimens in the study explained in the list of abbreviations

The Concrete Batching Plant (CBP) supplied all concrete mixture ingredients according to the quantity in the ACI-Code mix design [48]. All wooden forms were prepared, and the column specimens were cast. They were de-molded in 24 hours after casting and then cured with water; Figure 4 shows the column specimens after casting and de-mold.

2.4 Test setup and instrumentations

All column specimens were tested using the universal testing machine at the structural laboratory, as shown in Figure 5. Reinforced concrete columns underwent vertical testing under compressive concentric and eccentric loading until failure.

A monotonic load was applied using a hydraulic jack with a capacity of 2000 kN. The loading rate was 0.4 mm/min [53]**.** Several instrumentations were used to measure the deformations, axial load, and strain. Data loggers were used to record the measurements and dates for the test. Figure 6 shows the location of the applied load for the required eccentricity ratio. Four electronic LVDTs were installed to measure each column specimen's lateral and axial displacement until failure. Two LVDTs were placed at the middle height of the column in the opposite faces to measure the lateral displacement, and one LVDT was also placed at the mid-height but perpendicular to the others to measure the out-of-plane movement of the lateral displacement. Another LVDT was placed at the bottom end of the column to calculate the average axial displacement.

Strain gauges were placed on column steel and GFRP reinforcement before casting, and a concrete strain gauge was placed on the faces of the column at mid-height of the specimen before the test to measure the value of the strain occurring in concrete.

This study considered 3 eccentricity values (e) to investigate the behavior of the reinforcement concrete columns under concentric and eccentric loads: 0mm, 100mm, and 150mm. To achieve the required eccentricity value, the dimensions and location of the bearing rod steel were selected such that the distance from the center lines of the plate and the column section is equal to the intended eccentricity, as shown in Figure 6.

Figure 2. The wooden forms and reinforcement of concrete columns

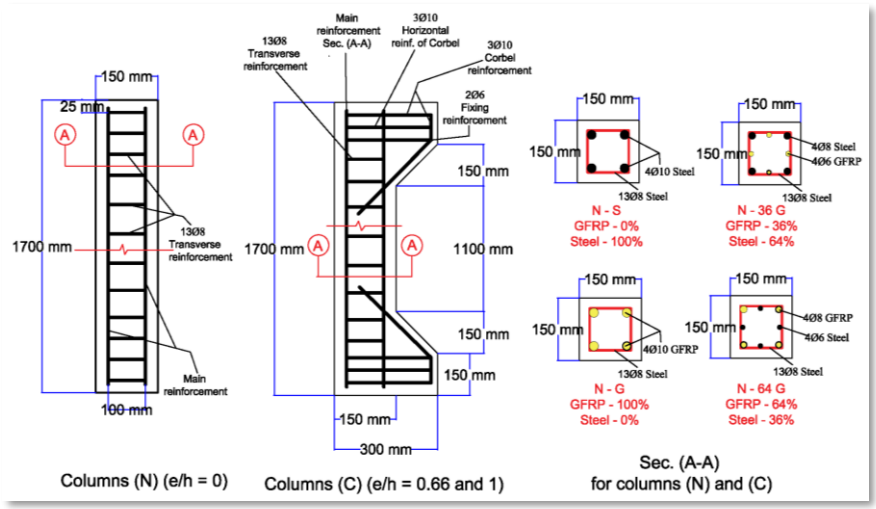

Figure 3. Dimension and reinforcement details of R.C. columns (N) and (C)

Table 4. Reinforcement details, ratios, eccentricity, and details of the R.C. columns (N) and (C)

Group No.	Coding	Corbel	Reinforcement Percentage of GFRP %	Reinforcement Percentage of steel %	Eccentricity value (e) mm	Eccentricity ratio(e/h)	Longitudinal reinforcement	Transverse reinforcement
1	N-S	no	0	100	0 mm	0	4Ø10 steel	13Ø8@100mm c/c
	N-G	no	100	0	0 mm	0	4Ø10 GFRP	13Ø8@100mm c/c
	N-36G	no	36	64	0 mm	0	4Ø8 steel & 4Ø6 GFRP	13Ø8@100mm c/c
	N-64G	no	64	36	0 mm	0	4Ø6 steel & 4Ø8 GFRP	13Ø8@100mm c/c
2	C1-S	yes	0	100	100 mm	0.66	4Ø10 steel	13Ø8@100mm c/c
	C1-G	yes	100	0	100 mm	0.66	4Ø10 GFRP	13Ø8@100mm c/c
	C1-36G	yes	36	64	100 mm	0.66	4Ø8 steel & 4Ø6 GFRP	13Ø8@100mm c/c
	C1-64G	yes	64	36	100 mm	0.66	4Ø6 steel & 4Ø8 GFRP	13Ø8@100mm c/c
3	C2-S	yes	0	100	150 mm	1	4Ø10 steel	13Ø8@100mm c/c
	C2-G	yes	100	0	150 mm	1	4Ø10 GFRP	13Ø8@100mm c/c
	C2-36G	yes	36	64	150 mm	1	4Ø8 steel & 4Ø6 GFRP	13Ø8@100mm c/c
	C2-64G	yes	64	36	150 mm	1	4Ø6 steel & 4Ø8 GFRP	13Ø8@100mm c/c

Figure 4. R.C. columns specimens

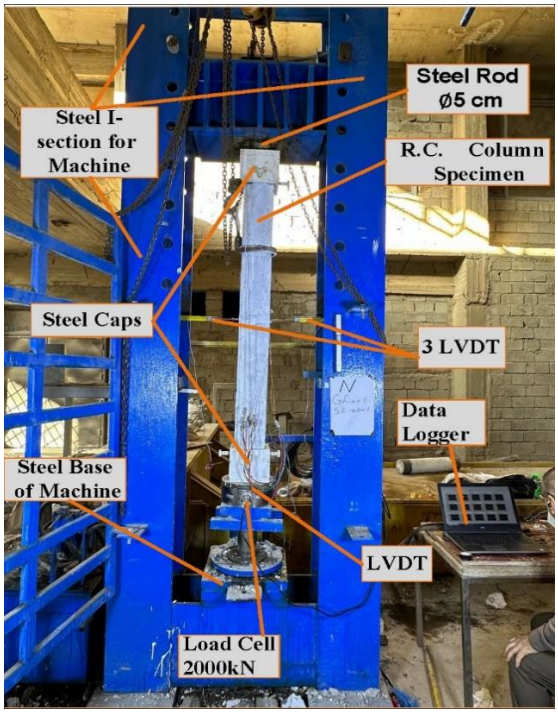

Figure 5. Test machine with all details used in the experimental test

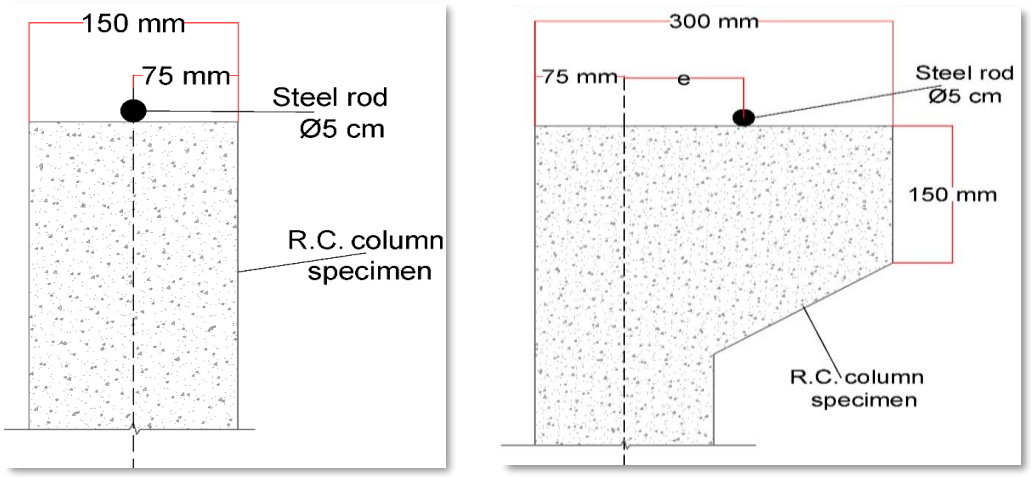

[a] e = 0 mm (e/h=0) [b] (e = 100 and 150 mm) (e/h= 0.66 and 1)

Figure 6. Location of the bearing rod steel used to achieve the required eccentricity ratio

3. Results and discussion

3.1 Failure mode

Figure 7 shows the modes of failure that occurred in the first group for the column specimens after the applied concentric compression load. the failures occurring from the applied load in these columns are concrete crushing failures at the first third of the column's height near regions where the concentric load is applied. For the column control specimen (N—S), the damage started with spalling in the concrete cover due to the initiated buckling in the longitudinal steel reinforcement. For the control specimen (N—G), The damage is noted in the regions where the concentric load is applied, followed by kinking in GFRP bars that occur in the compression zone, as shown in Figure 7-b and Figure 8. The main reason for the kinking in the GFRP bars is that, generally, the compressive strength of fiber-reinforced polymer (FRP) bars varies depending on the type of FRP material used, the GFRP bars have low compressive strength ranging between 300 to 600 MPa; therefore, the bars in the compression zone kink simultaneously in concrete crushing. This observation was in agreement with [54]. Also, for columns partially reinforced with GFRP bars (N—36 G), the GFRP bars were first affected by compressive stress, and the kinking phenomena were observed in the GFRP bars in the compression zone. However, the columns partially reinforced GFRP bars (N—64 G); the damage was noted at first in the GFRP bars, which were kinking because they were affected by compressive stress from the applied load.

Figure 9 shows the failure modes in the second group for the columns subjected to an eccentric compression loading (e/h=0.66). The failure modes in these columns occurred clearly from the corbel's end instructs with the column to the mid-height of the column. Initially, a few cracks were observed in the tension zone after the load was applied, and then, with the increase in load, initial spalling in concrete was observed. The final failure step occurred due to a sudden crash in the concrete. For the columns containing GFRP bars, as partially or fully reinforced, the final failure step occurred due to concrete crushing, and kinking was noted in the GFRP bars, as shown in Figure 9 - b, followed by a sudden drop in the column's compressive strength. Figure 10 shows the failure modes in the third group for the columns tested under an eccentric load with an eccentricity ratio (e/h=1). The failure modes in these columns in this group occurred at the end first third of the height. from the corbel's end instructs with the column to the mid-height of the column. firstly, the cracks were observed in the tension zone, and then, with the increase in load applied, concrete spalling occurred,

and failure was observed due to concrete crushing followed by a sudden drop in the column's compressive strength. But for the columns containing GFRP bars, as partially or fully reinforced, the final failure step occurred due to concrete crushing, and kinking was noted in the GFRP bars. Therefore, the failure in these columns under concentric and eccentric load results from approaching a buckling failure up to the middle height of the specimen in the weakest region by crushing before buckling. Kinking in GFRP bars also occurs in the compression zone. In this study, the type of failure in GFRP bars due to compression stress indicates that the damage destroyed the bars completely. Moreover, GFRP bars can sustain available tensile strength, which enhances the column's bending moment.

Failure of columns containing GFRP bars is more serious than failure of control columns with steel rebars, because of GFRP bars due to compression stress damaged and destroyed completely

a) N - S b) N - G c) N – 36 G d) N - 64 G

Figure 7. Failure modes for R. C. columns specimens with eccentricity ratio e/h=0

Figure 8. Kinking in GFRP bars that occur in the compression zone for the specimens [N-G]

a) C1 - S b) C1 - G c) C1 - 36 G d) C1 – 64 G e) C1 – 64 G

Figure 9. Failure modes for R. C. columns specimens with eccentricity ratio e/h=0.66

a) C2 - S b) C2 - G c) C2 - 36 G d) C2 – 64 G e) C2 – 64 G

Figure 10. Failure modes for R. C. columns specimens with eccentricity ratio e/h=1

3.2 Axial Load – Displacement Behaviour

Table 5 illustrates the reinforcement ratios of columns with GFRP bars and conventional steel rebars. Moreover, the experimental test results include the concentric and eccentric compression load failure and the average maximum axial displacement at failure load for all tested column specimens.

Figure 11-14) present the load—axial displacement relationships for all specimens.

The average axial displacement value for columns specimens tested under eccentric load at (e/h) ratio (0.66 and 1) decreases by (75%) and (94.4%) compared with the control specimen in the same reinforcement in concentric load with (e/h=0) (N - S). The average axial displacement under eccentric load decreases by (46.4%) and (57.7%) compared with (e/h) ratio (0) for (N - G), decreases by (68.2%) and (76.2%) compared with (e/h) ratio (0) for (N – 36 G). And decreases by (46.1%) and (52%) compared (e/h) ratio (0) for (N – 64 G). The ratios reduced the bearing capacity of the columns in the groups in which the GFRP bars were used as partial or complete replacements in the main reinforcement. Moreover, the percentage of dropping the bearing capacity for columns with GFRP bars tested under eccentric load reduces with increasing the ratio of GFRP bars.

In the first group of column specimens subjected to concentrated loads, the axial failure load decreases with increased reinforcement ratio with GFRP bars. When the full reinforcement with GFRP bars, the failure load decreases by (18.55%) with an increase in the axial displacement by (17.11) compared to the control specimens. However, when the 36% reinforcement with GFRP bars, the failure load decreases by (4.38%) with an increase in the axial displacement by (5.7%), as well as the 64% reinforcement with GFRP bars, the failure load decreases by (10.75%) with an increase in the axial displacement by (8.57%).

In the second group of column specimens subjected to eccentric load with eccentricity ratio e/h (0.66), the full reinforcement with GFRP bars, the failure load decreases by (25.95%) with an increase in the axial displacement by (40%) compared to the control specimens. However, when the 36% reinforcement with GFRP bars, the failure load decreases by (17.02%) with an increase in the axial displacement by (10%), as well as the 64% reinforcement with GFRP bars, the failure load decreases by (38.65%) with an increase in the axial displacement by (30%).

And the third group of column specimens subjected to eccentric load with eccentricity ratio e/h (1), the full reinforcement with GFRP bars, the failure load decreases by (21.31%) with an increase in the axial displacement by (44.44%) compared to the control specimens. However, when the 36% reinforcement with GFRP bars, the failure load decreases by (19.35%) with an increase in the axial displacement by (16.66%), as well as the 64% reinforcement with GFRP bars, the failure load decreases by (54.16%) with an increase in the axial displacement by (38.88%).
Based on the experimental results for the axial load, the designer needs to be conservative when using GFRP bars as the main reinforcement in the R.C. columns and uses them when the design of moments and high average axial displacement is desired.

Figure 15 clearly shows axial load failure with the axial displacement relationship for column specimens under concentric load with (e/h=0). In general, it was observed that increasing the internal reinforcement ratios of GFRP bars leads to a decrease in the failure load and increased deformation compared with the control specimen (N—S). The failure loads for columns with partial reinforcement with GFRP bars are higher than those with full GFRP because GFRP, unlike steel rebars, cannot resist the stresses in the compression zone during loading [54]. The response of the control specimens (N - S) under concentric load started with liners in the first stage. Then, the non-linear behavior was observed in the second stage up to failure. In contrast to specimens containing partial reinforcement with GFRP bars, the behaviors were nearly linear, and in the specimens containing fully GFRP bars as reinforcement, the behaviors were linear; this behavior depends on the type of material. Steel rebars are known to be characterized by linear behavior in the elasticity stage and then plasticity as a second stage begins, in which the behavior is non-linear. This is unlike the behavior of GFRP bars, characterized by

linear or close-to-linear behavior during the loading stages up to failure.

Based on the above results, the axial failure load decreased with an increased reinforcement ratio with GFRP bars. In contrast, the average axial displacement began increasing with an increased reinforcement ratio with GFRP bars.

Table 5: Experimental results: values recorded during the tests R.C. columns specimens (N) and (C)

Group No.	Coding	Corbel	Reinforcement Percentage of GFRP %	Reinforcement Percentage of steel %	Eccentricity value (e) mm	Eccentricity ratio (e/h)	Max load Failure [kN]	Moment at load failure [kN.m]	Max axial displacement [mm]
1	N-S	no	0	100	0 mm	0	690	0	3.5
	N-G	no	100	0	0 mm	0	582	0	4.1
	N-36G	no	36	64	0 mm	0	661	0	3.7
	N-64G	no	64	36	0 mm	0	623	0	3.8
2	C1-S	yes	0	100	100 mm	0.66	165	16.5	2.0
	C1-G	yes	100	0	100 mm	0.66	131	13.1	2.8
	C1-36G	yes	36	64	100 mm	0.66	141	14.1	2.2
	C1-64G	yes	64	36	100 mm	0.66	119	11.9	2.6
3	C2-S	yes	0	100	150 mm	1	74	11.1	1.8
	C2-G	yes	100	0	150 mm	1	61	9.15	2.6
	C2-36G	yes	36	64	150 mm	1	62	9.3	2.1
	C2-64G	yes	64	36	150 mm	1	48	7.2	2.5

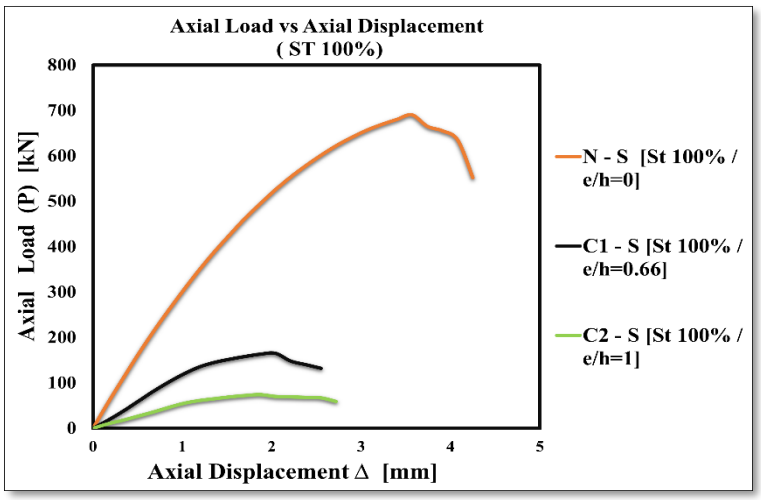

Figure 11. Axial load vs. axial displacement relationship column specimens [N - S] with different eccentricity ratios e/h=0, e/h=0.66, and e/h=1

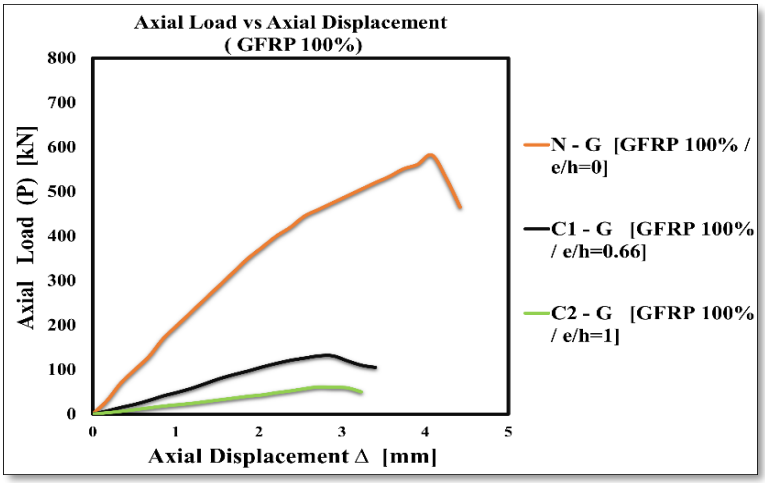

Figure 12. Axial load vs. axial displacement relationship column specimens [N - G] with different eccentricity ratios e/h=0, e/h=0.66, and e/h=1

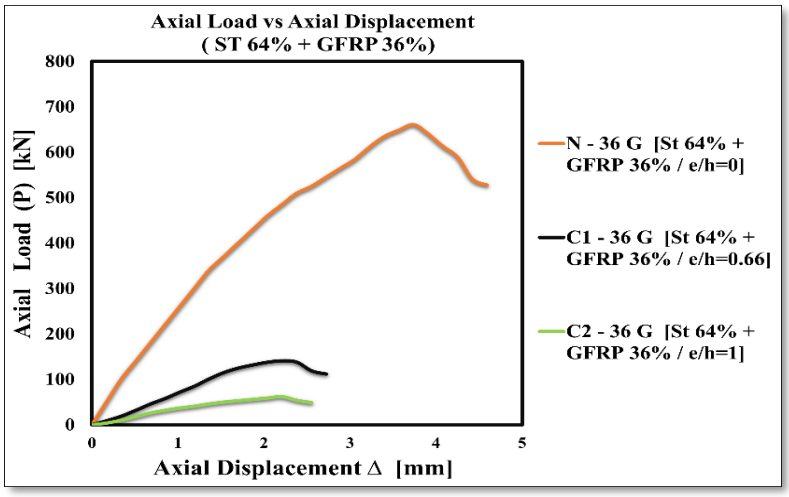

Figure 13. The axial load vs. axial displacement relationship columns specimens [N—36 G] with different eccentricity ratios e/h=0, e/h=0.66, and e/h=1

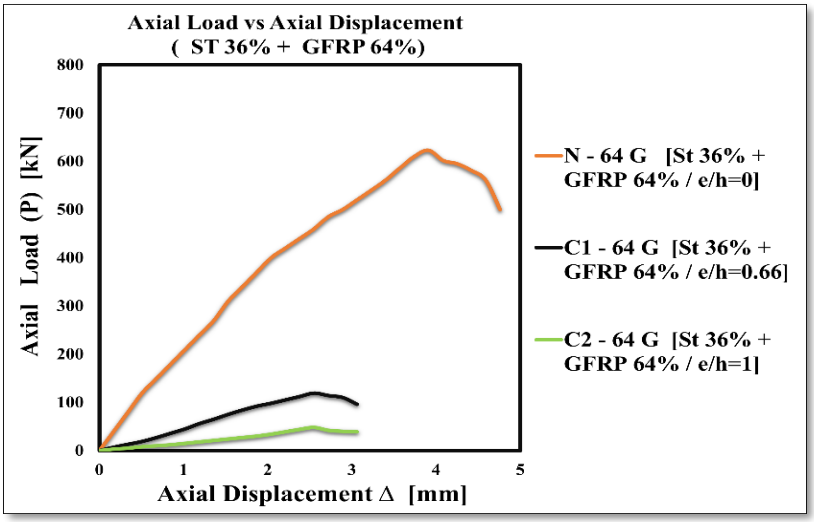

Figure 14. The axial load vs. axial displacement relationship columns specimens [N—64 G] with different eccentricity ratios e/h=0, e/h=0.66, and e/h=1

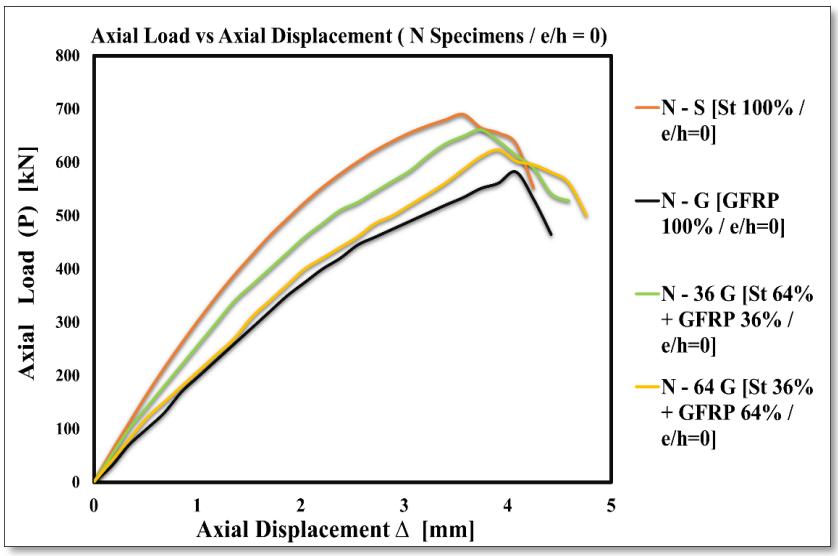

Figure 15. Axial load vs. axial displacement relationship for columns specimens [N] with e/h=0.

3.3 Interaction diagram behaviour

Figure 16 shows the theoretical interaction diagram for a column fully reinforced with steel bars according to ACI 318 [55,56], a column fully reinforced with GFRP bars (100%) according to ACI 440.1R [54], and a column partially reinforced with GFRP bars (36% and 64%) according to Nanni et al.[50,57]. It can be noted from Figure 16 that the theoretical axial load failure value for column specimens tested under concentric load decreases by (22.89%) for the (N-G) (GFRP 100%) specimens compared with the theoretical axial load failure of control specimen (N - S). decreases by (13.17%) for the (N – 36 G) (St 64% +GFRP 36%) compared with the control specimen and decreases by (7%) for the (N – 64 G) (St 36% +GFRP 64%) also compared with the control specimen.

The ultimate axial load and bending moment for the column reinforcement partially by GFRP bars decreased when the replacement ratio of internal reinforcement with GFRP bars increased. Moreover, when the column is fully reinforced with GFRP bars, the bending moment improves compared to partial replacement and control specimens with decreased axial load failure. It is very important to mention that the balanced condition of the column reinforced with fully GFRP bars is near the horizontal axis where the axial load is equal to zero (the bending moment axis) [50,57] in contrast to the balanced failure in the column reinforced by steel or partially GFRP bars. It was concluded that the existing steel and GFRP bars simultaneously affect the distribution of the stresses in the main reinforcement because, In the tension zone, the tensile stress is distributed on the GFRP and steel bars based on the modulus of elasticity and tensile strength of materials, it known that the modulus of elasticity of steel rebars higher the modulus of elasticity of GFRP bars about 4 times and lower in tensile strength about 3 times. However, in the compression zone, only the concrete and steel bars sustained the compressive stress and neglected the GFRP bars because of the GFRP bar's low compressive strength for the load applied.

The reduction in the values of the load axial as the replacement ratios of GFRP bars increase is because the tensile strength of GFRP bars is higher than the tensile strength of steel rebars, but the modulus of elasticity is lower, as mentioned above. The compressive stresses in GFRP bars are small or can be neglected in the compression zone; all these specifications for the reinforcement materials affect the stress distribution and the failure load [54,58].

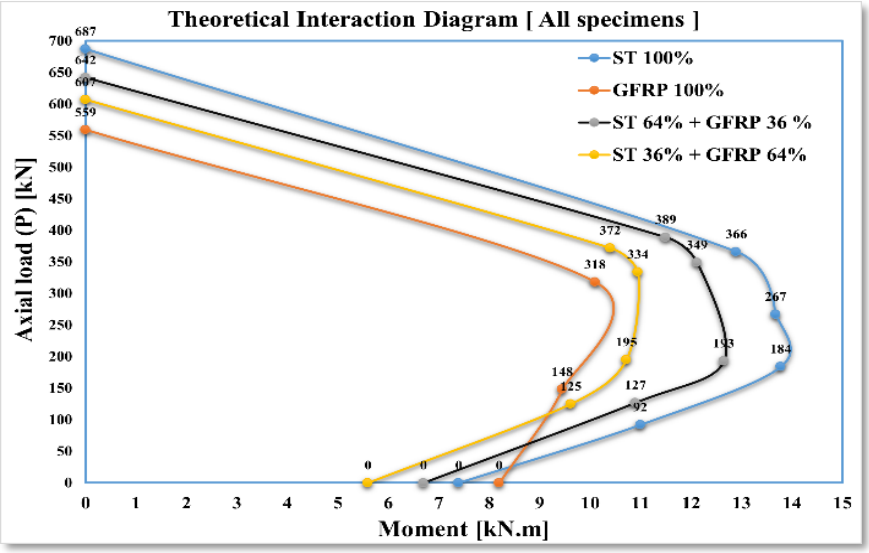

Figure 16. Theoretical interaction diagram for column specimens [54,55,57,59]

Table 5 shows the reinforcement ratios of columns with GFRP bars and conventional steel rebars. The experimental test results include the concentric and eccentric compression load failure, the bending moment, and the average maximum axial displacement at failure load for all tested column specimens. Figures (17- 20) show the column's theoretical interaction diagram

with the experimental results. The different eccentricity ratios (e/h) (0, 0.66, and 1) were plotted for comparison as results from the column tested.

From the curves plotted in the Figures, it is important to mention that theoretical interaction diagrams were drawn without reduction factors recommended by the ACI community. The ACI code always applies reduction factors to the strength values through the design to achieve the required safety factor for structural elements. All reduction factors have been canceled by calculating the theoretical interaction diagram for the column specimens to compare the experimental results that appear during the test accurately with the results drawn theoretically.

Figures 17 compares the theoretical interaction diagram and the experimental results for the control column [N -S]. The experimental results of the concentric load capacity are slightly higher than the theoretical concentric load, which means the design, according to the ACI code, is conservative and takes a factor of safety because it uses an overall capacity reduction factor to reflect the overall variation in all material properties. Because of this, different capacity reduction factors are used in different areas of design.

Furthermore, the experimental results of the eccentric load capacity with different ratios of eccentricities show that all points of the experimental results fall outside the boundaries of the theoretical interaction diagram. Moreover, the theoretical result is very close to the experimental results except for the balance condition; it was found that the theoretical result is conservative.

Figure 18 compares the theoretical interaction diagram and the experimental results for the column fully reinforced with GFRP bars (100%). The experimental results of the concentric load capacity for the column [N-G] are higher than the theoretical concentric load capacity by (4%).

Moreover, the experimental results of the eccentric load capacity with different ratios of eccentricities for columns reinforced with 100% GFRP bars, show that all points of the experimental results fall outside the boundaries of the theoretical interaction diagram and very close to it, and can show clearly from Figure 18, except for the experimental balance condition is away from the theoretical interaction diagram. This means the design, according to the ACI code, is very conservative in the balanced condition failure for the column containing GFRP bars because a balanced condition is reached when the compression strain in the concrete becomes limited, and the tensile strength of GFRP yields simultaneously. Concrete failure occurs at the same time as GFRP yields. Since the tensile strength of GFRP bars is about three times greater than the tensile strength of normal steel rebars, the tensile strength of the GFRP bars is reduced in the theoretical calculations of the interaction diagram. Figure 19 compares the theoretical interaction diagram and the experimental results for the column partially reinforced with 36% GFRP bars and 64% normal steel rebars; the experimental results of the concentric load capacity for the column [N- 36G] are higher than the theoretical concentric load capacity by (2.9%). Howover, the experimental results of the eccentric load capacity with different ratios of eccentricities for columns reinforced with 36% GFRP bars and 64%, show that all points of the experimental results fall outside the boundaries of the theoretical interaction diagram and near it, except for the experimental balance condition is away from the theoretical interaction diagram. As mentioned earlier, when calculating a theoretical interaction diagram, the tensile strength of the GFRP bars is being reduced, and the results of the ACI code it is very conservative.

Figure 20 compares the theoretical interaction diagram and the experimental results for the column partially reinforced with 64% GFRP bars and 36% normal steel rebars, the experimental results of the concentric load capacity for the column [N- 64G] are higher than the theoretical concentric load capacity by (2.5%). Moreover, the experimental results of the eccentric load capacity with different ratios of eccentricities for columns reinforced with 64% GFRP bars and 36%, show that all points of the experimental results fall outside the boundaries of the theoretical interaction diagram and close to it, except for the experimental balance condition is away from the theoretical interaction diagram. As mentioned earlier, when calculating a theoretical interaction diagram, the tensile strength of the

GFRP bars is being reduced, and the results of the ACI code it is very conservative.

Based on the results showed that the theoretical result in some regions is conservative. However, the theoretical and experimental results for the pure axial load capacity were very close. The failure loads for specimens with partial reinforcement are higher than those containing fully GFRP. Still, this ratio can be used when moments and high vertical displacement are desired in design.

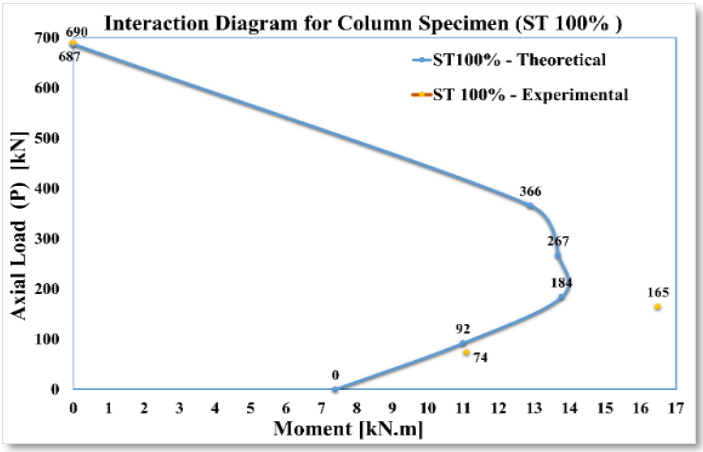

Figure 17. Comparison between the theoretical interaction diagram for column [N -S] and the experimental results for different eccentricities (e/h = 0), (e/h = 0.66), and (e/h = 1)

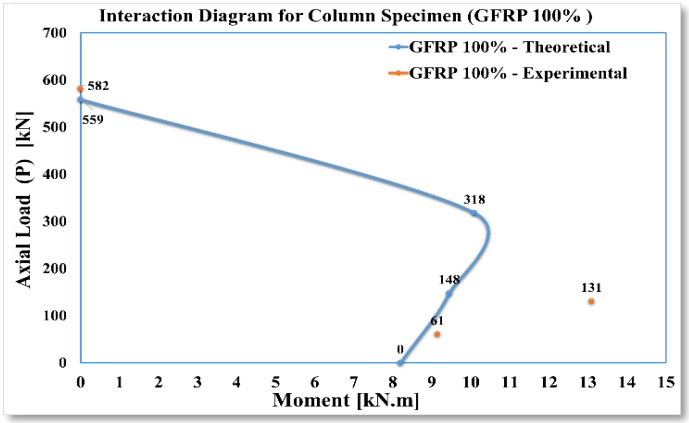

Figure 18. Comparison between the theoretical interaction diagram for column [N - G] and the experimental results for different eccentricities (e/h = 0), (e/h = 0.66), and (e/h = 1).

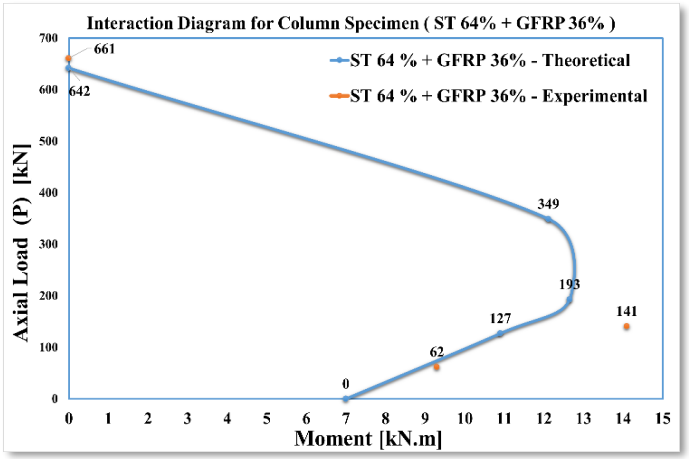

Figure 19. Comparison between the theoretical interaction diagram for column [N – 36 G] and the experimental results for different eccentricities (e/h = 0), (e/h = 0.66), and (e/h = 1)

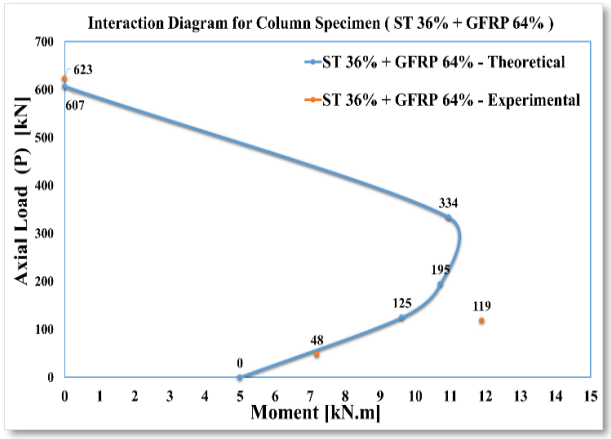

Figure 20. Comparison between the theoretical interaction diagram for column [N – 64 G] and the experimental results for different eccentricities (e/h = 0), (e/h = 0.66), and (e/h = 1)

4 Conclusions

This study prepared and tested 12 reinforced concrete columns under concentric and eccentric loads with different eccentric ratios (e/h) (0, 0.66, and 1). These specimens were partially and fully reinforced with GFRP bars in ratios (36%, 64%, and 100%), and the control specimen was reinforced with conventional steel rebars. The mode of failure, theoretical and experimental strength capacity, and average axial displacement. were obtained. The following conclusions can be drawn based on the test results reported in the present study:

- Longitudinal reinforcement type and ratios dominated column failure regarding gradual concrete cover spalling and kinking of the GFRP bars at the maximum applied load.
- A reinforced column with full GFRP bars enhances the bending moment due to balanced conditions approaching the horizontal axis.
- Concrete columns reinforced with full GFRP bars exhibited lower strength capacity than partially replaced GFRP bars and steel reinforcement concrete columns. This reduction in column capacity must be considered in the design.
- The column specimens subjected to concentrated loads, the axial failure load decreases with increased reinforcement ratio with GFRP bars. When the full reinforcement with GFRP bars, the failure load decreases by (18.55%) with an increase in the axial displacement by (17.11) compared to the control specimens. Moreover, when the 36% reinforcement with GFRP bars, the failure load decreases by (4.38%) with an increase in the axial displacement by (5.7%), as well as the 64% reinforcement with GFRP bars, the failure load decreases by (10.75%) with an increase in the axial displacement by (8.57%).
- The column specimens subjected to concentrated loads, the axial failure load decreases with increased reinforcement ratio with GFRP bars. When the full reinforcement with GFRP bars, the failure load decreases by (18.55%) with an increase in the axial displacement by (17.11) compared to the control specimens. Moreover, when the 36% reinforcement with GFRP bars, the failure load decreases by (4.38%) with an increase in the axial displacement by (5.7%), as well as the 64% reinforcement with GFRP bars, the failure load decreases by (10.75%) with an increase in the axial displacement by (8.57%).
- The column specimens subjected to eccentric load with eccentricity ratio e/h (0.66), the full reinforcement with GFRP bars, the failure load decreases by (25.95%) with an increase in the axial displacement by (40%) compared to the control specimens. Moreover, when the 36% reinforcement with GFRP bars, the failure load decreases by (17.02%) with an

increase in the axial displacement by (10%), as well as the 64% reinforcement with GFRP bars, the failure load decreases by (38.65%) with an increase in the axial displacement by (30%).

- The column specimens subjected to eccentric load with eccentricity ratio e/h (1), the full reinforcement with GFRP bars, the failure load decreases by (21.31%) with an increase in the axial displacement by (44.44%) compared to the control specimens. Moreover, when the 36% reinforcement with GFRP bars, the failure load decreases by (19.35%) with an increase in the axial displacement by (16.66%), as well as the 64% reinforcement with GFRP bars, the failure load decreases by (54.16%) with an increase in the axial displacement by (38.88%).
- the theoretical axial load failure value for column specimens tested under concentric load decreases by (22.89%) for the (N-G) (GFRP 100%) specimens compared with the theoretical axial load failure of control specimen (N - S). decreases by (13.17%) for the (N – 36 G) (St 64% +GFRP 36%) compared with the control specimen and decreases by (7%) for the (N – 64 G) (St 36% +GFRP 64%) also compared with the control specimen.

List of Abbreviations

Symbol	Meaning
ACI	American Concrete Institute
ASTM	American Society of Testing Materials
R.C.	Reinforced Concrete
GFRP	Glass Fiber Reinforced Polymer
I.Q.S.	Iraqi specifications stander
N-S	Normal column without corbel under concentric load reinforced with steel rebars.
N-G	Normal column without corbel under concentric load reinforced with fully GFRP bars.
N-36G	Normal column without corbel under concentric load reinforced with 64% steel rebars and 36% GFRP bars.
N-64G	Normal column without corbel under concentric load reinforced with 36% steel rebars and 64% GFRP bars.
C1-S	Column with corbel under eccentric load (e=100mm) reinforced with steel rebars.
C1-G	Column with corbel under eccentric load (e=100mm) reinforced with fully GFRP bars.
C1-36G	A column with a corbel under eccentric load (e=100mm) is reinforced with 64% steel rebars and 36% GFRP bars.
C1-64G	Column with corbel under eccentric load (e=100mm) reinforced with 36% steel rebars and 64% GFRP bars.
C2-S	Column with corbel under eccentric load (e=150mm) reinforced with steel rebars.
C2-G	A column with corbel under eccentric load (e=150mm) reinforced with fully GFRP bars.
C2-36G	A column with corbel under eccentric load (e=150mm) reinforced with 64% steel rebars and 36% GFRP bars.
C2-64G	A column with corbel under eccentric load (e=150mm) reinforced with 36% steel rebars and 64% GFRP bars.

List of notations

Symbol	Meaning	Units
f_y	Yield stress of steel reinforcement bars	**MPa**
fu	The ultimate strength of reinforcement bars	**MPa**
f_{cu}	Cubic compressive strength of concrete at 28 days	**MPa**
ϕ	Steel bar diameter	**mm**
Es	Steel modulus of elasticity	**MPa**
P	Ultimate load	**kN**
Δ	Displacement at failure load	**mm**

Reference

[1] A. J. H. Alshimmeri, "Structural Behavior of Confined Concrete Filled Aluminum Tubular (CFT) Columns under Concentric Load," *Journal of Engineering*, vol. 22, no. 8, pp. 125–139, 2016.

[2] A. H. Al-Zuhairi, A. H. A. Al-Ahmed, A. N. Hanoon, and A. A. Abdulhameed, "Structural behavior of reinforced hybrid concrete columns under biaxial loading," *Latin American Journal of Solids and Structures*, vol. 18, p. e390, 2021.

[3] P. K. Mallick, *Fiber-reinforced composites: materials, manufacturing, and design*. CRC press, 2007.

[4] A. El-Sayed, E. El-Salakawy, and B. Benmokrane, "Shear strength of one-way concrete slabs reinforced with fiber-reinforced polymer composite bars," *Journal of Composites for Construction*, vol. 9, no. 2, pp. 147–157, 2005.

[5] B. Benmokrane, E. El-Salakawy, A. El-Ragaby, and T. Lackey, "Designing and testing of concrete bridge decks reinforced with glass FRP bars," *Journal of Bridge Engineering*, vol. 11, no. 2, pp. 217–229, 2006.

[6] H. R. Hamilton Iii and C. W. Dolan, "Flexural capacity of glass FRP strengthened concrete masonry walls," *Journal of Composites for Construction*, vol. 5, no. 3, pp. 170–178, 2001.

[7] A. H. Al-Zuhairi, A. H. A. Al-Ahmed, A. N. Hanoon, and A. A. Abdulhameed, "Structural behavior of reinforced hybrid concrete columns under biaxial loading," *Latin American Journal of Solids and Structures*, vol. 18, p. e390, 2021.

[8] D. H. Deitz, I. E. Harik, and H. Gesund, "One-way slabs reinforced with glass fiber reinforced polymer reinforcing bars," *Special Publication*, vol. 188, pp. 279–286, 1999.

[9] M. Theriault and B. Benmokrane, "Effects of FRP reinforcement ratio and concrete strength on flexural behavior of concrete beams," *Journal of composites for construction*, vol. 2, no. 1, pp. 7–16, 1998.

[10] H. A. Toutanji and M. Saafi, "Flexural behavior of concrete beams reinforced with glass fiber-reinforced polymer (GFRP) bars," *Structural Journal*, vol. 97, no. 5, pp. 712–719, 2000.

[11] S. H. Alsayed, "Flexural behaviour of concrete beams reinforced with GFRP bars," *Cem Concr Compos*, vol. 20, no. 1, pp. 1–11, 1998.

[12] Q. Shakir and B. Abd, "RETROFITTING OF SELF COMPACTING RC HALF JOINTS WITH INTERNAL DEFICIENCIES BY CFRP FABRICS," *J Teknol*, vol. 82, pp. 49–62, Oct. 2020.

[13] Q. Shakir and Y. Yahya, "Stitching of T-deep beams with large openings by CFRP sheets and NSM steel bars," *Pollack Periodica*, Apr. 2024.

[14] Q. M. Shakir and S. D. Abdlsaheb, "Rehabilitation of partially damaged high strength RC corbels by EB FRP composites and NSM steel bars," *Structures*, vol. 38, pp. 652–671, 2022.

[15] A. U. Syed and A. Goldack, "Slenderness limit for GFRP reinforced concrete columns based on axial force ratio," *Eng Struct*, vol. 298, p. 117026, 2024.

[16] L. Xiao, H. Hu, S. Peng, Z. Du, and C. Xu, "Compression behavior of GFRP reinforced hybrid fibre reinforced concrete short columns subjected to eccentric loading," *Constr Build Mater*, vol. 393, p. 131985, 2023.

[17] A. Hadhood, H. M. Mohamed, F. Ghrib, and B. Benmokrane, "Efficiency of glass-fiber reinforced-polymer (GFRP) discrete hoops and bars in concrete columns under combined axial and flexural loads," *Compos B Eng*, vol. 114, pp. 223–236, 2017.

[18] M. N. S. Hadi and J. Youssef, "Experimental investigation of GFRP-reinforced and GFRP-encased square concrete specimens under axial and eccentric load, and four-point bending test," *Journal of Composites for Construction*, vol. 20, no. 5, p. 04016020, 2016.

[19] T. A. Hales, C. P. Pantelides, and L. D. Reaveley, "Experimental evaluation of slender high-strength concrete columns with GFRP and hybrid reinforcement," *Journal of Composites for Construction*, vol. 20, no. 6, p. 04016050, 2016.

[20] H. Gao, L. Wang, B. Chen, and M. Yan, "Axial compressive behavior of GFRP tube-reinforced concrete-steel double skin tubular columns," *Journal of Building Engineering*, vol. 75, p. 106973, 2023.

[21] S. Natarajan and S. S. Selvan, "Experimental study on axial compression behaviour of glass fibre reinforced polymer (GFRP) wrapped nano material concrete columns," *Mater Today Proc*, vol. 39, pp. 748–757, 2021.

[22] CSA S806-12 code, "Design and Construction of Building Structures with Fibre-Reinforced Polymers," 2017.

[23] M. Motavalli and C. Czaderski, "FRP composites for retrofitting of existing civil structures in Europe: State-of-the-art review," in *international conference of composites & polycon*, American Composites Manufacturers Association Tampa, FL, USA, 2007, pp. 17–19.

[24] E. Alsuhaibani *et al.*, "Compressive and Bonding Performance of GFRP-Reinforced Concrete Columns," *Buildings*, vol. 14, p. 1071, Apr. 202.

[25] K. Khorramian and P. Sadeghian, "Behavior of slender GFRP reinforced concrete columns," in *Structures Congress 2019*, American Society of Civil Engineers Reston, VA, 2019, pp. 88–99.

[26] H. M. M. and B. B. Mohammad Z. Afifi, "Axial Capacity of Circular Concrete Columns Reinforced with GFRP Bars and Spirals," *Journal of Composites for Construction*, vol. 18, no. 1, Sep. 2013.

[27] C. C. Choo, I. Harik, and H. Gesund, "Strength of rectangular concrete columns reinforced with fiber-reinforced polymer bars," vol. 103, pp. 452–459, May 2006.

[28] A. Mirmiran, M. Shahawy, and T. Beitleman, "Slenderness Limit for Hybrid FRP-Concrete Columns," *Journal of Composites for Construction - J COMPOS CONSTR*, vol. 5, Feb. 2001, doi: 10.1061/(ASCE)1090-0268(2001)5:1(26).

[29] W. Lu, X. Q. Li, and D. Zhou, "Experimental study on corrosion resistance of GFRP bars body," *Journal of Mechanical Engineering Research and Developments*, vol. 39, pp. 826–831, Jan. 2016.

[30] J. Mao, H. Zhang, J. Lv, D. Jia, and S. Ao, "Mechanical Properties and Corrosion Mechanism of GFRP Rebar in Alkaline Solution," *Key Eng Mater*, vol. 665, pp. 217–220, Sep. 2015, doi: 10.4028/www.scientific.net/KEM.665.217.

[31] A. Kramarchuk, B. Ilnytskyy, O. Lytvyniak, and Y. Famulyak, "Strengthening prefabricated reinforced concrete roof beams that are damaged by corrosion of concrete and reinforcement," *IOP Conf Ser Mater Sci Eng*, vol. 708, p. 012060, Dec. 2019.

[32] Z. Guo, M. Ye, Y. Chen, and X. Chen, "Experimental study on compressive behavior of concrete-filled GFRP tubular stub columns after being subjected to acid corrosion," *Compos Struct*, vol. 250, p. 112630, Jun. 2020.

[33] R. Z. Hamed and H. F. Hassan, "Structural Behavior of GFRP-RC Slender Columns Under Various Eccentricity Loading Conditions," *Civil and Environmental Engineering*, 2023.

[34] Z. Pu, X. Lv, Y. Liu, H. Zhang, Y. Wang, and S. A. Sheikh, "Eccentric behaviour of GFRP-reinforced square columns with composite spiral ties," *Journal of Building Engineering*, vol. 79, p. 107915, 2023.

[35] H. Al-Thairy and M. A. Al-Hamzawi, "Behavior of Eccentrically Loaded Slender Concrete Columns Reinforced with GFRP Bars," in *Journal of Physics: Conference Series*, IOP Publishing, 2021, p. 012218.

[36] Dr. M. Elchalakani, G. Ma, F. Aslani, and W. Duan, "Design of GFRP-reinforced rectangular concrete columns under eccentric axial loading," *Magazine of Concrete Research*, vol. 69, pp. 1–13, May 2017.

[37] M. Elchalakani and G. Ma, "Tests of glass fibre reinforced polymer rectangular concrete columns subjected to concentric and eccentric axial loading," *Eng Struct*, vol. 151, pp. 93–104, 2017.

[38] M. Guérin, H. Mohamed, B. Benmokrane, C. Shield, and A. Nanni, "Effect of Glass Fiber-Reinforced Polymer Reinforcement Ratio on the Axial–Flexural Strength of Reinforced Concrete Columns," *ACI Struct J*, vol. 115, Jul. 2018.

[39] A. Hadhood, H. M. Mohamed, F. Ghrib, and B. Benmokrane, "Efficiency of glass-fiber reinforced-polymer (GFRP) discrete hoops and bars in concrete columns under combined axial and flexural loads," *Compos B Eng*, vol. 114, pp. 223–236, 2017.

[40] A. Hadhood, H. M. Mohamed, and B. Benmokrane, "Experimental study of circular high-strength concrete columns reinforced with GFRP bars and spirals under concentric and eccentric loading," *Journal of Composites for Construction*, vol. 21, no. 2, p. 04016078, 2017.

[41] A. Hadhood, H. M. Mohamed, and B. Benmokrane, "Axial load–moment interaction diagram of circular concrete columns reinforced with CFRP bars and spirals: Experimental and theoretical investigations," *Journal of Composites for Construction*, vol. 21, no. 2, p. 04016092, 2017.

[42] M. Guérin, H. Mohamed, B. Benmokrane, A. Nanni, and C. Shield, "Eccentric Behavior of Full-Scale Reinforced Concrete Columns with Glass Fiber-Reinforced Polymer Bars and Ties," *ACI Struct J*, vol. 115, Mar. 2018.

[43] M. G. Gouda, H. M. Mohamed, A. C. Manalo, and B. Benmokrane, "Experimental investigation of concentrically and eccentrically loaded circular hollow concrete columns reinforced with GFRP bars and spirals," *Eng Struct*, vol. 277, p. 115442, 2023.

[44] S. Xiaobin, G. Xianglin, L. Yupeng, C. Tao, and Z. Weiping, "Mechanical Behavior of FRP-Strengthened Concrete Columns Subjected to Concentric and Eccentric Compression Loading," *Journal of Composites for Construction*, vol. 17, no. 3, pp. 336–346, Jun. 2013.

[45] X. Song, X. Gu, Y. Li, T. Chen, and W. Zhang, "Mechanical behavior of FRP-strengthened concrete columns subjected to concentric and eccentric compression loading," *Journal of Composites for Construction*, vol. 17, no. 3, pp. 336–346, 2013.

[46] K. Khorramian and P. Sadeghian, "Experimental and analytical behavior of short concrete columns reinforced with GFRP bars under eccentric loading," *Eng Struct*, vol. 151, pp. 761–773, 2017.

[47] N. Siddiqui, H. Abbas, T. Almusallam, A. Binyahya, and Y. Al-Salloum, "Compression behavior of FRP-strengthened RC square columns of varying slenderness ratios under eccentric loading," *Journal of Building Engineering*, vol. 32, p. 101512, 2020.

[48] ACI PRC-211.1-91, *Standard Practice for Selecting Proportions for Normal, Heavyweight, and Mass Concrete (Reapproved 2009)*, ACI PRC-211.1-91. 2009.

[49] BS EN 12390-1:2000, "Testing hardened concrete - Shape, dimensions and other requirements for specimens and moulds," *BSI*, 2000.

[50] A. Nanni, A. De Luca, and H. J. Zadeh, *Reinforced concrete with FRP bars: Mechanics and design*. CRC press, 2014.

[51] H. Tobbi, A. S. Farghaly, and B. Benmokrane, "Concrete Columns Reinforced Longitudinally and Transversally with Glass Fiber-Reinforced Polymer Bars.," *ACI Struct J*, vol. 109, no. 4, 2012.

[52] W. Xue, F. Peng, and Z. Fang, "Behavior and Design of Slender Rectangular Concrete Columns Longitudinally Reinforced with Fiber-Reinforced Polymer Bars.," *ACI Struct J*, vol. 115, no. 2, 2018.

[53] M. Panjehpour, N. Farzadnia, R. Demirboga, and A. Ali, "Behavior of high-strength concrete cylinders repaired with CFRP sheets," *Journal of Civil Engineering and Management*, vol. 22, pp. 56–64, Jan. 2016.

[54] ACI 440.1r-15, "aci 440.1r-15," *ACI Code*, 2015.

[55] ACI Code Standard, *Building Code Requirements for Structural Concrete (ACI 318-19)*, 2019th ed. 2019.

[56] D. Darwin, C. W. Dolan, and A. H. Nilson, *Design of concrete structures*, vol. 2. McGraw-Hill Education New York, NY, USA: 2016.

[57] H. Jawaheri Zadeh and A. Nanni, "Design of RC columns using glass FRP reinforcement," *Journal of Composites for Construction*, vol. 17, pp. 294–304, Jun. 2013, doi: 10.1061/(ASCE)CC.1943-5614.0000354.

[58] A. S. F. Hany Tobbi and Brahim Benmokrane, "Concrete Columns Reinforced Longitudinally and Transversally with Glass Fiber-Reinforced Polymer Bars," *ACI Struct J*, vol. 109, no. 4, 2012.

[59] A. H. Nilson, D. Darwin, and C. W. Dolan, *Design of Concrete Structures*. McGraw-Hill Higher Education, 2010. [Online]. Available: https://books.google.iq/books?id=13rPngEACAAJ